Ionic Polymers Based on Dextran: Hydrodynamic Properties in Aqueous Solution and Solvent Mixtures

Luminita Ghimici,*,† Marieta Nichifor,† and Bernhard Wolf‡

"Petru Poni" Institute of Macromolecular Chemistry, Aleea Grigore Ghica Voda 41A, 700487 Iasi, Romania, and Institute of Physical Chemistry, University of Mainz, Welder-Weg 13, D-55099 Mainz, Germany

Received: January 23, 2009; Revised Manuscript Received: April 29, 2009

Hydrodynamic properties of a series of ionic polysaccharides with different charge density but the same molecular weight have been evaluated in salt-free aqueous solution and aqueous/organic solvent mixtures by means of capillary viscometry. The polyelectrolytes investigated contain quaternary ammonium salt groups, *N*-ethyl-*N*,*N*-dimethyl-2-hydroxypropylammonium chloride, attached to a dextran backbone. The experimental viscometric data have been plotted in terms of the Wolf method. The results show that the experimental data fit well with this model and allow the calculation of intrinsic viscosities and other hydrodynamic parameters, which provide new information about the dependence of the polyion conformation on its polyion charge density as well as on solvent composition.

Introduction

Solution properties of polyelectrolytes exhibit interesting behavior that differs considerably from uncharged macromolecules or low molar mass electrolytes. The origin of this specificity and high complexity of these systems lies in the combination of properties derived from long-chain molecules with those derived from charge interactions. The major impediment in the study of polyelectrolyte solutions arises from the long-range Coulomb interactions between charges leading to a rich variety of effects, which are not found in a solution of neutral polymers. Thus, unlike neutral polymers, reduced viscosity increases monotonously with an increase in dilution, making impossible the extrapolation to zero concentration of the $\eta_{sp}/c-c$ curve (Huggins plot) in order to obtain the intrinsic viscosity, $[\eta]$.[1] Fuoss and Strauss explained this increase of the reduced viscosity (η_{sp}/c or η_{red}) by progressively enhanced dissociation of the ionizable groups and, hence, intensification of the intramolecular repulsion along each macromolecular coil.[2] They described this behavior with an empirical equation: $\eta_{sp}/c = A/1 + Bc^{1/2}$. The inverse equation suggests that a linear relationship between c/η_{sp} and $c^{1/2}$ should yield a straight line with a slope of B/A and an intercept of $1/A$. The Fuoss and Strauss equation is based on the following assumptions: (i) the continuous increase of the reduced viscosity with dilution is solely due to the intramolecular interactions, and (ii) the conformation of the chains at infinite dilution is rodlike. Both assumptions have been called into question over time. Thus, experimental results showed that the curves η_{sp}/c vs c reached a maximum at very low polyelectrolyte concentrations for aqueous, as well as nonaqueous, solutions.[3−9] The existence of the maximum has been first assigned to a polyion final state of expansion in a finite concentration range, after which η_{red} will then decrease with dilution like neutral polymers. These maxima were sometimes perceived as an artifact, due to the impurities that may be present in the solvent,[10] the ionic contribution resulting from the autodissociation of water at very high dilution, or the adsorption of polymer onto the glass capillary wall, which causes an upbending of the reduced viscosity in the extremely dilute concentration regime even for neutral polymer solutions.[11] However, experimental studies performed on solutions of very high purity confirmed the presence of this maximum for various polyelectrolytes.[12−17] These results as well as those obtained for other systems, such as telechelic ionomers,[18,19] ionic latex particles of NaPSS,[20,21] spherical and branched poly(styrenesulfonate),[22,23] a stiff-chain cationic poly(*p*-phenylene) polyelectrolyte,[24] led to other explanations for the reduced viscosity increase and its maximum: the formation of relatively large solvated clusters,[16] the long-range Coulombic interactions,[16] the intermolecular electrostatic interactions between charged particles called the secondary electroviscous effects,[21,25,26] and the competition between screening of the electrostatic interactions that scale as $c^{-1/2}$ and decreasing intermolecular distances that scale as $c^{-1/3}$.[26]

Irrespective of the given explanation, the occurrence of peaks makes the extrapolation of viscometric data to infinite dilution according to the Fuoss equation inappropriate. This empirical relation does not address such maxima.

Then, other equations were proposed to describe the viscometric behavior of polyelectrolyte solutions. Notable among them are Juan−Dougherty−Stivala,[27] Martin,[28] Yang,[29] and Rushing and Hester.[30] Fedors' equation[31] modified by Rao,[32] verified for neutral polymers, has been successfully extended to some polyelectrolytes in both water[33−36] and water/organic solvent mixtures.[35,37−39] Despite the substantial amount of work on the intrinsic viscosity of polyelectrolyte solutions, it is still difficult to find equations that depict their viscosity behavior in the whole range of concentration.

Recently, a purely phenomenological approach for the determination of $[\eta]$, which avoided extrapolations and, hence, complications in the above-mentioned methods, has been presented.[40,41] According to this model, $[\eta]$ can be determined either from the initial slope of the $\ln \eta_{rel}-c$ plot, which is independent of any model assumptions, or by means of one of the following equations:

* To whom correspondence should be addressed. Tel: +40-232-260333. Fax: +40-232-211299. E-mail: lghimici@icmpp.ro.
† "Petru Poni" Institute of Macromolecular Chemistry.
‡ University of Mainz.

10.1021/jp900690f CCC: $40.75
Published on Web 05/14/2009

$$\ln \eta_{rel} = \frac{c[\eta] + Bc^2[\eta][\eta]^*}{1 + Bc[\eta]} \quad (1)$$

$$\ln \eta_{rel} = A(1 - e^{-([\eta]-[\eta]^{\pm})} \pm c/A) + [\eta]^{\pm}c \quad (2)$$

where A and B represent system specific constants, and $[\eta]^*$ and $[\eta]^{\pm}$ are characteristic specific hydrodynamic volumes.

In order to interpret the viscosity data, some parameters were also introduced, such as $\{\eta\}$ is the specific hydrodynamic volume at a given polymer concentration c, and $\{\eta\}/[\eta]$ is the ratio between the specific hydrodynamic volume at a given polymer concentration c and that at infinite dilution. This ratio provides information on the changes in the hydrodynamic volume of individual macromolecules induced by the presence of other polymers. The value of this ratio can be obtained from eq 3

$$\frac{\{\eta\}}{[\eta]} = \frac{1 + 2Brc[\eta] + B^2r^2c^2[\eta]^2}{1 + 2Bc[\eta] + B^2c^2[\eta]^2} \quad (3)$$

where $r = [\eta^*]/[\eta]$ and $c[\eta]$ is a dimensionless reduced concentration.

So far, this model has been applied successfully for salt-free aqueous solutions of poly(*N*-butyl-4-vinylpyridinium bromide) samples with a different quaternization degree[40] and of sodium poly(styrenesulfonate)[41] as well as for salt solutions of sodium poly(styrenesulfonate).[40]

The goal of the present work was to describe the viscosity behavior of some cationic polysaccharides based on dextran, D40-Et*X*, in salt-free aqueous solutions and water/methanol mixtures using this method. This allowed us to establish the dependence of the hydrodynamic volume of a macroion on the polymer concentration, charge density, and solvent composition.

Experimental Part

Materials. Cationic polysaccharides with pendent quaternary ammonium groups were synthesized by chemical modification of dextran samples (Sicomed S.A., Bucharest, Romania) with a molar mass of $M_w = 40$ kg/mol and $M_w/M_n = 1.12$, as determined by capillary viscometry and static light scattering in aqueous solution. The procedure for the synthesis of these polymers has been described elsewhere.[42] The polymers were extensively purified by repeated precipitation and dialysis against 0.1 N HCl and water and finally recovered as a white powder by lyophilization. The chemical structure, shown in Scheme 1, was proved by ^{1}H NMR and elemental analysis. The polymer's code is D40-Et*X*, where D means dextran, 40 is the dextran molar mass in kg/mol, Et stands for ethyl and is the substituent at the amino group of the D40-Et*X*, and $X = DS \pm 2$ mol %. DS is the degree of substitution and is expressed as moles of amino groups per 100 glucopyranosidic units; $DS = 100x/(x + y)$, where x and y are the molar fraction of substituted and unsubstituted glucosidic units, respectively. The content in amino groups (DS) was determined from nitrogen content (elemental analysis) and chloride ion content (potentiometric titration with 0.02 N $AgNO_3$ aqueous solution). Table 1 lists several properties of the cationic polymers.

Methods. Viscometric measurements of the polyelectrolyte solutions were carried out with an Ubbelohde viscometer at 25 °C. All polyelectrolytes were dissolved in highly purified deionized water from a Milli-Q PF (Millipore, Switzerland).

SCHEME 1: General Chemical Structure of Polycations Based on Dextran (D40-Et*X*)

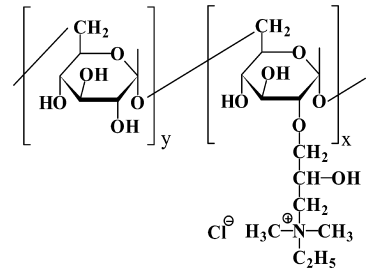

TABLE 1: Characteristics of the Polycation Samples

sample D40-Et*X*	Cl_i,[a] mequiv/g	*X*, mol % quaternary amino group	*b*,[b] nm	ξ,[c] 20 °C, water
D40-Et18	0.95	18	2.86	0.25
D40-Et35	1.59	35	1.47	0.48
D40-Et74	2.59	74	0.70	1.01
D40-Et94	2.96	94	0.55	1.30

[a] Cl_i refers to the chloride ion content. [b] *b* is the average spacing between two vicinal ionized groups on the polyion, based on a repeating unit length of 0.515 nm for the D-glycopyranose unit.[43] [c] ξ is the charge density parameter, calculated according to refs 44 and 45.

All viscosity measurements were repeated at least twice in order to check the reliability of the data which was within ±3%.

Results and Discussion

D40-Et*X* in Pure Water. Charge Density Dependence of Viscosities. Examination of the Huggins plots for the unmodified dextran sample (Dex40) (Figure 1a) and for the quaternized derivatives of dextran (Figure 1b) led to the following findings: (i) a linear decrease of the reduced viscosity values with dilution in the case of the unmodified dextran sample, as expected for a neutral polymer; (ii) a clear polyelectrolyte effect, i.e., a well-defined upward curvature appeared for all of the quaternized dextran samples due to intra- and intermolecular repulsive electrostatic interactions; (iii) a higher content of the quaternized units in the copolymer at constant degree of polymerization, brought about an increase of η_{red}, which means an increase of the coil dimension in solution.

Usually, dilute neutral polymer solution $[\eta]$ can be obtained by means of the Huggins equation (4):

$$\frac{\eta_{sp}}{c} = [\eta](1 + k_H c[\eta] + ...) \quad (4)$$

where k_H is the Huggins coefficient, which quantifies the specific hydrodynamic interactions between the polymer and solvent. For the unmodified dextran sample, the extrapolation of η_{sp}/c to zero concentration gives $[\eta] = 18.66$ mL g^{-1} (Figure 1a, line). As the $\eta_{sp}/c-c$ curves for cationic dextran samples (Figure 1b) could not be extrapolated to zero concentration in order to obtain $[\eta]$, we used eq 1 to evaluate the experimental viscosity data (Figure 2b, solid lines). This equation was also applied to the experimental viscosity data of the unmodified dextran sample (Figure 2a, solid line). The values of the parameters in eq 1 are taken as adjustable parameters, and the values corresponding to the best fit of this equation to experimental data are summarized in Table 2. In the same table are included the

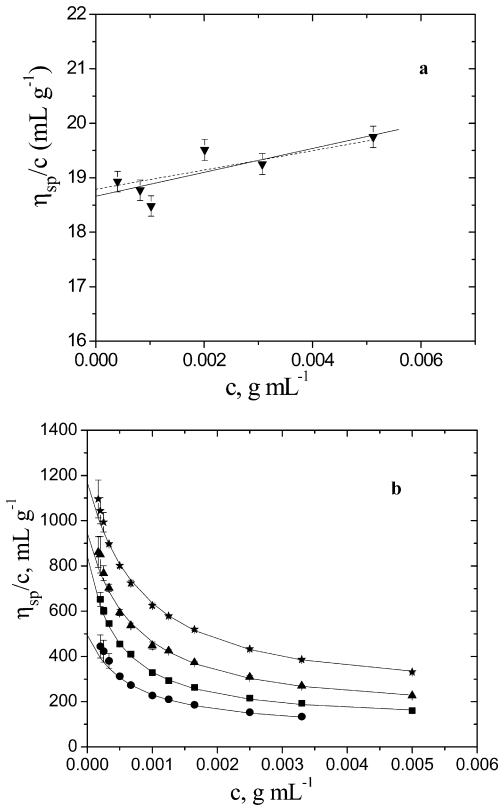

Figure 1. (a) Reduced viscosity, η_{sp}/c, dependence on the polyelectrolyte concentration, c, for Dex40 (symbol, the experimental data; solid line, linear fit to experimental data; dashed line, Huggins plot with prefixed $k_H = 0.5$ using the following equation: $\eta_{sp}/c = 18.79\ (1 + 0.5 \times 18.79c)$, where 18.79 is the intrinsic viscosity obtained by means of the Wolf equation). (b) Reduced viscosity, η_{sp}/c, dependence on the polyelectrolyte concentration, c: (circle) D40-Et18; (square) D40-Et35; (triangle) D40-Et74; (star) D40-Et94. Symbols are the evaluation of the original experimental data. Lines are modeled according to eq 1 by means of the parameters in Table 2.

TABLE 2: Parameters of Eq 1 and the Intrinsic Viscosity, [η], Obtained by the Rao Equation for the Unmodified Dextran Sample, Dex40, and Cationic Polysacharides, D40-Et*X*

sample	[η], mL g^{-1}	[η]*, mL g^{-1}	B	[η]$_{Rao}$, mL g^{-1}
Dex40	18. 9	0	0	19
D40-Et18	495.0	41.5	3.5	534
D40-Et35	847.7	60.9	3.0	813
D40-Et74	947.0	63.2	1.9	990
D40-Et94	1170.0	77.8	1.4	1204

intrinsic viscosity values previously obtained by means of the Rao method.[35]

The results demonstrate that all of the calculated curves (lines) coincided well with the experimental points and confirm that eq 1 is appropriate to describe the viscosity behavior of samples under study (Figure 2a,b). This is also enforced by the Huggins plots calculated with the parameters in Table 2 by means of eq 1 (Figure 1b, lines). Except for polymer concentrations lower than 5×10^{-4} g mL^{-1}, the lines drawn in Figure 1b matched well with the experimental data points. Moreover, according to this approach, eqs 5 and 6 should yield $k_H = 0.5$ for neutral polymers, as in this case $B = [\eta]^* = 0$.

$$k = \left(1 - \frac{[\eta]^*}{[\eta]}\right)B \tag{5}$$

$$k = \frac{1}{2} - k_H \tag{6}$$

The Huggins evaluation of the unmodified dextran sample using the [η] and B values obtained from the ln $\eta_{rel}-c$ plot (Figure 2a, Table 2) and translating B into k_H reads $\eta_{sp}/c = 18.79\ (1 + 0.5 \times 18.79c)$ (Figure 1a, dashed line). The close values for [η] obtained with the original Huggins evaluation and the present used model is remarkable.

Also obvious is the strong influence of the sample's charge density (or degree of substitution DS) and of the concentration on the viscosity parameters. When the charge density increases, the intrinsic viscosity values increase up to 10 times than that of the unmodified dextran sample (Table 2, Figure 3). This is consistent with the fact that the presence of charges leads to a larger expansion of the polymer chains at infinite dilution. Furthermore, the dependencies of [η] and [η*] on DS are similar in shape (Figure 3), with a "flat" region around 50 mol %, which could be explained by a more significant effect of charges at lower and higher DS.

Also worthy to note is the observation that the intrinsic viscosities obtained by means of eq 1 agree well with those resulting from Rao's model (Table 2).

Regarding the hydrodynamic interaction parameter B, one notices that it passes a maximum as a function of DS; according to the relation between k_H and B, this corresponds to a minimum in k_H. The observed behavior can be rationalized in terms of

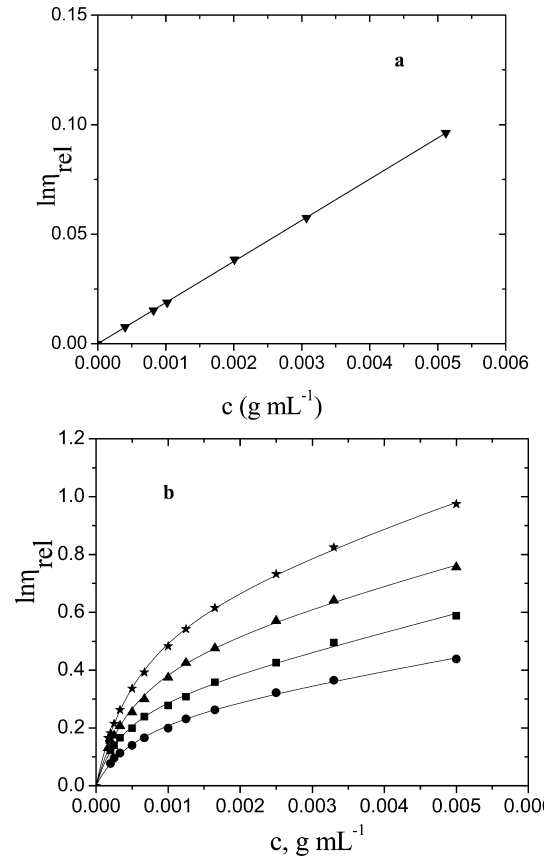

Figure 2. (a) Relative viscosities, ln η_{rel}, dependence on the polyelectrolyte concentration, c, for Dex40. Line was calculated according to eq 1 by means of the parameters of Table 2. (b) Relative viscosities, ln η_{rel}, dependence on the polyelectrolyte concentration, c: (circle) D40-Et18; (square) D40-Et35; (triangle) D40-Et74; (star) D40-Et94. Lines were calculated according to eq 1 by means of the parameters of Table 2.

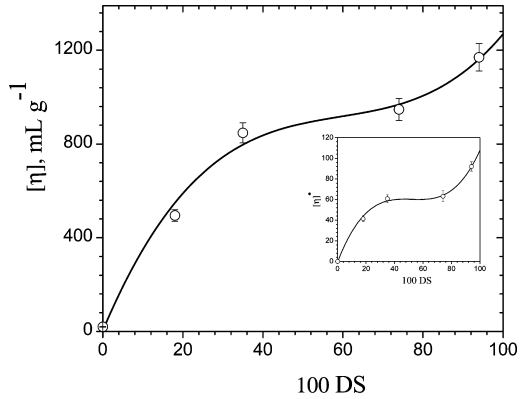

Figure 3. Substitution degree, DS, dependence of $[\eta]$ and $[\eta]^*$ (inset). The lines are adjusted to a third-order polynomial.

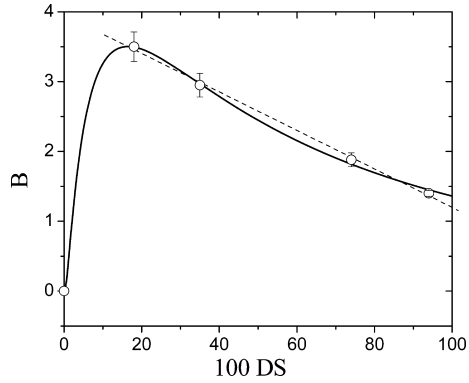

Figure 4. Substitution degree, DS, dependence of B (eq 1). The broken line is the linear fit to experimental data. The full line represents a log-normal dependence.

the so-called "pull-along" effect,[46] which results from the thermodynamic preference of contacts between polymer segments over contacts between solvent molecules and polymer segments; this phenomenon contributes to a viscosity increase via the formation of a weak physical network and leads to higher k_H and lower B values, respectively. In terms of the pull-along effect, the maximum in B signifies the least probability for the formation of intersegmental polymer contacts. It is, furthermore, noteworthy that $B = f(DS)$ is almost linear once the maximum has been passed (Figure 4, dashed line).

The influence of the polymer concentration is more clearly seen in Figure 5 where the reduced polymer concentration dependence of the reduced specific hydrodynamic volume is depicted.

The curves were calculated by means of eq 3 taking $[\eta]$, $[\eta]^*$, and B values from Table 2. The decrease of $\{\eta\}/[\eta]$ from 1 ($\{\eta\}/[\eta] = 1$ at $[\eta]c = 0$, as $\{\eta\} = [\eta]$) with increasing reduced polymer concentration is observed for all cationic samples over the whole reduced concentration range studied. The steep decrease of $\{\eta\}/[\eta]$ and, hence, of the relative coil volume (up to around 0.2 for D40-Et18 and 0.4 for D40-Et94) takes place up to $[\eta]c = 0.5$ and is followed by a slower decrease upon further increase of the reduced polymer concentration. This finding can be explained as follows. It is well-known that the conformation of polyelectrolyte chains is mainly influenced by their charge density and counterion dissociation. At high dilution, the counterions are far away from the polyion, and the chains become more extended due to the ionic repulsive forces between the charged groups of the macroion: the higher the charge density, the more extended polymer chains. According to this approach, as the polymer concentration increases,

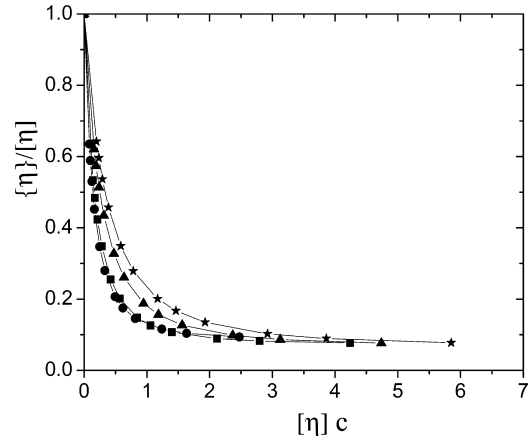

Figure 5. Reduced specific hydrodynamic volumes, $\{\eta\}/[\eta]$, as a function of the reduced polymer concentrations, $[\eta]c$: (circle) D40-Et18; (square) D40-Et35; (triangle) D40-Et74; (star) D40-Et94.

the polyelectrolyte coils shrink below the maximum extension they attain at $c = 0$, because of the progressive screening of electrical charges that results from the additional solute molecules. In addition, one has to mention that, when the polyelectrolyte concentration increases, the environmental ionic strength will increase, which also determines the electrostatic shielding of the charged groups and, hence, the shrinkage of the chains. The relative coil shrinkage with increasing concentration is similar for all cationic polymers, with only small attenuation with increasing charge density (Figure 5). The great reduction of the hydrodynamic volume of D40-Et74 and D40-Et94 was quite surprising because of their highest charge density and, hence, the most extended chains. However, a closer examination showed us this finding could be plausible. The charge density parameter of D40-Et74 and D40-Et94, $\xi = 1.0$ and 1.3, respectively (Table 1), is greater than or equal to the critical charge density parameter, $\xi_c = 1$ ($\xi_c = |z_c|^{-1}$, where z_c is the counterion valence). In this case, within the Manning theory, the counterion condensation takes place.[44,45] On the basis of the Stevens and Kremer results, obtained by computer simulation,[47] as well as on the theoretical ones of Schiessel and Pincus,[48] we may infer that the counterion condensation also contributes to the shrinkage of the polyion chains even at high dilution. Even so, there were still many charges on the chain whose intrachain Coulombic repulsions determined the lower degree of relative coil shrinkage for the D40-Et74 and D40-Et94 samples compared to the other cationic polysaccharides. All these relationships are more clearly illustrated in Figure 6 where the variation of $\{\eta\}/[\eta]$ vs ξ is plotted for different reduced polycation concentrations.

The extent to which an augmentation of the charge density increases the reduced specific hydrodynamic volume depends on the reduced polymer concentration $c[\eta]$. The higher this concentration becomes, the lower is the effect. Also visible in this graph is the coil shrinkage resulting from an increase in $c[\eta]$ at constant ξ.

D40-Et*X* in Solvent Mixtures. Solvent Composition Dependence of Viscosities. It is well-known that the solubility of a polyelectrolyte in a solvent is determined by both the affinity of the solvent for the neutral polymer and the solvation of the ionic species. For a given solvent, these two contributions may be additive or subtractive, and in the latter case, the solubility, obviously, depends on their relative importance.

The behavior of polyelectrolytes in nonaqueous solution or in mixed solvents can provide important information about

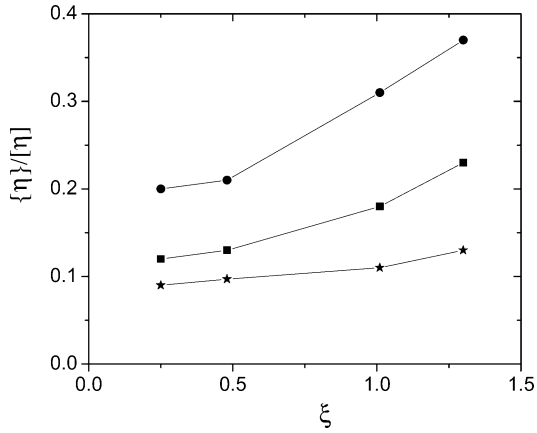

Figure 6. Reduced specific hydrodynamic volumes, $\{\eta\}/[\eta]$, as a function of the charge density, ξ, for different reduced polymer concentrations, $c[\eta]$: (circle) 0.5; (square) 1; (star) 2.

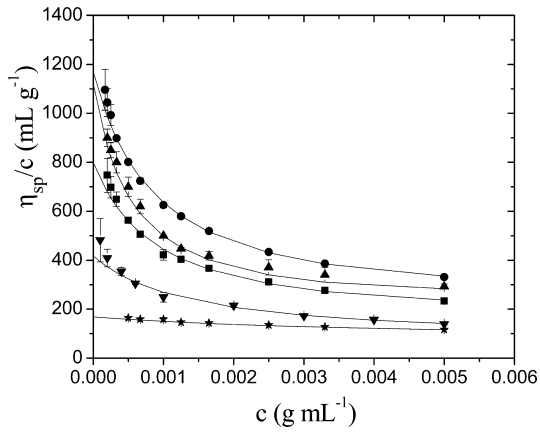

Figure 7. Reduced viscosity, η_{sp}/c, dependence on the polyelectrolyte concentration, c, for D40-Et94 in a water/methanol mixture: (solid circle) water; (triangle) 90/10; (square) 50/50; (inverted triangle) 10/90; (star) methanol. Lines are modeled according to eq 1 by means of the parameters in Table 3.

electrostatic interactions useful for practical activities. Therefore, in the second part of this paper, we examine the experimental viscosity data of D40-Et94 in methanol and solvent mixtures of water/methanol in terms of the present model.

The plots of Figure 7 show that the reduced viscosity behavior for D40-Et94 in the water/methanol mixtures followed the same tendency as in water. Although less pronounced, polymers behave like polyelectrolytes because the ionizable groups along the backbone can also dissociate in these polar solvent mixtures. Furthermore, the experimental data clearly show differences, induced by modifying the solvent quality; for a given concentration, the reduced viscosity decreases with a decrease in the dielectric constant of the solvent. This may have the following explanations: (i) less polar solvents enable less ionizable groups to dissociate and, consequently, lead to lower intra/intermolecular repulsive interactions between the charged groups, and (ii) according to Manning,[44,45] when the dielectric constant of the solvent decreases, ξ increases. This might lead to a larger amount of condensed counterions and, thus, to a decrease in polyion-chain size. Both phenomena determined by the dielectric constant decrease can act simultaneously.

Figure 8 shows the curves calculated when applying eq 1 to the experimental data points. The values of the parameters in eq 1 are summarized in Table 3 together with the intrinsic viscosity values previously obtained by means of the Rao method.[35]

TABLE 3: Parameters of Eq 1 and the Intrinsic Viscosity, [η], Obtained by the Rao Equation for D40-Et94 in Water/Methanol Solvent Mixtures

mixture water/methanol, % vol	[η], mL g^{-1}	[η]*, mL g^{-1}	B	$[\eta]_{Rao}$, mL g^{-1}
100/0	1170.00	77.8	1.40	1204
90/10	1124.6	99	1.99	537
50/50	800	66.73	1.8	529
10/90	417.5	37.62	2.15	507
0/100	168.2	34.1	1.58	157

Similar to the results obtained in water, this model is capable of describing the viscosity behavior of D40-Et94 in solvent mixtures; all of the calculated curves (lines) agree well with the experimental data points irrespective of the solvent composition. This again is confirmed by the Huggins representation of the curves calculated with the parameters in Table 3 by means of the eq 1 (Figure 7, lines). Except for polymer concentrations lower than 2×10^{-4} g mL^{-1}, the lines drawn in Figure 7 matched well with the experimental data points.

The lower $[\eta]$ values of D40-Et94 with increasing methanol content in the mixture point to the reduction of the hydrodynamic dimension of the macroion coils as the dielectric constant of the solvent decreases (Table 3 and Figure 9). This plot provides a nonlinear dependence of $[\eta]$ versus solvent mixture composition. The agreement between the intrinsic viscosity values obtained by means of both methods was noticed only for the pure solvents, water, and methanol.

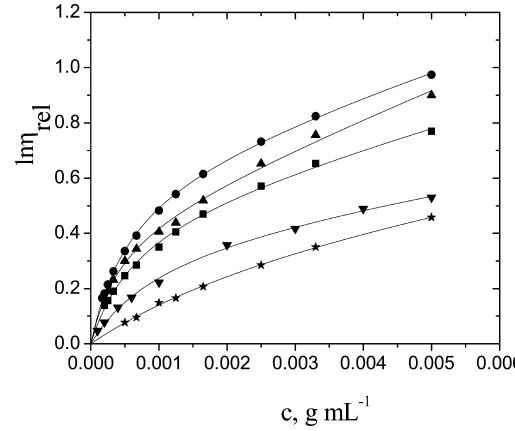

Figure 8. Relative viscosities, ln η_{rel}, as a function of the polymer concentrations, c, for D40-Et94 in a water/methanol mixture: (solid circle) water; (triangle) 90/10; (square) 50/50; (inverted triangle) 10/90; (star) methanol. Lines calculated according to eq 1 by means of the parameters of Table 3.

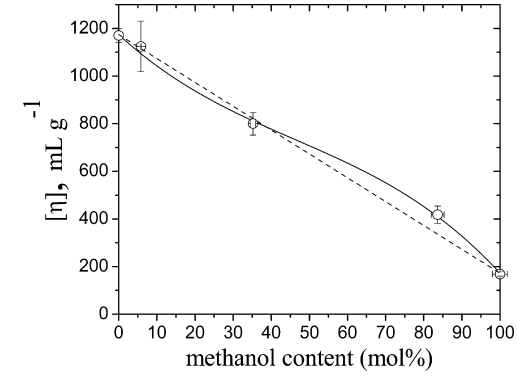

Figure 9. Intrinsic viscosities, $[\eta]$, dependence on the methanol content, mol %.

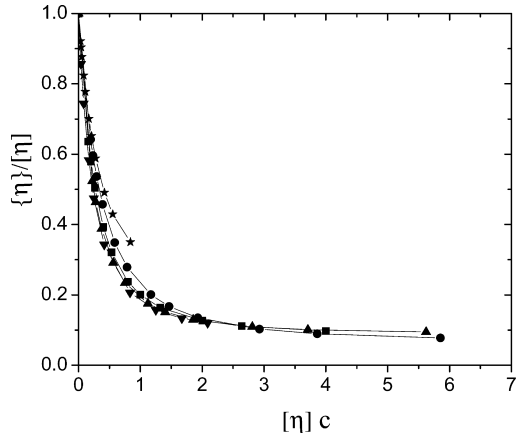

Figure 10. Reduced specific hydrodynamic volumes, $\{\eta\}/[\eta]$, as a function of the reduced polymer concentrations, $[\eta]c$, for D40-Et94 in a water/methanol mixture: (solid circle) water; (triangle) 90/10; (square) 50/50; (inverted triangle) 10/90; (star) methanol.

Figure 10 shows that in water/methanol mixtures the $\{\eta\}/[\eta]$ ratio (calculated by means of eq 3 taking $[\eta]$, $[\eta]^*$, and B values from Table 3) decreases rapidly as the reduced concentration increases; the coils of D40-Et94 shrink more than half for $[\eta]c < 0.5$ and remain almost constant for $[\eta]c > 2$. One should also mention that the degree of relative coil shrinkage with increasing concentration is less pronounced in pure methanol, maybe due to the already very coiled conformation of the polymer in this solvent.

Conclusions

In this paper, we have investigated the hydrodynamic properties of some cationic polysaccharides based on dextran in salt-free solutions in the light of the Wolf approach. The study presented here considers simultaneously a variety of parameters such as polymer concentration, charge density, and solvent composition. We have used a series of cationic polymers with a well-controlled chemical structure, which could supply reliable relationships between hydrodynamic properties and polymer chemical composition. The concentration dependences of viscosities of the present polyelectrolyte solutions can be described by means of the Wolf model in the whole range of polymer and solvent compositions. On the basis of this model, we could quantify several parameters describing the conformation and hydrodynamic volume of the polycations in the absence of salts: intrinsic viscosity, hydrodynamic interaction parameter B (a measure of polymer−polymer segment interactions), and reduced specific hydrodynamic volume (which quantify the hydrodynamic volume deviation from the maximum extended form at infinite dilution). The results can be summarized as follows:

(1) The intrinsic viscosities increase with increasing charge density and are up to ten times higher than that of the unmodified dextran sample. Decreasing the dielectric constant of the solvent leads to a decrease in intrinsic viscosity.

(2) By increasing charge density, the hydrodynamic interaction parameter reaches a maximum, then decreases almost linearly.

(3) The extent to which an augmentation of the charge density increases the reduced specific hydrodynamic volume depends on the reduced polymer concentration $c[\eta]$. The higher this concentration becomes, the lower is the effect. The lower $[\eta]$ values of D40-Et94 with increasing methanol content in the mixture point to the reduction of the hydrodynamic dimension of the macroions as the dielectric constant of the solvent decreases. A nonlinear dependence of $[\eta]$ versus solvent mixture composition was observed.

All these experimental data provide new information about the balance of interactions between polymer segments and solvent molecules and among the polymer segments, as well as the preponderance of intra- or intermolecular polymer segment interactions, as a function of polymer concentration and environmental characteristics.

References and Notes

(1) Dobrynin, A. V.; Colby, R. H.; Rubinstein, M. *Macromolecules* **1995**, *28*, 1859.
(2) Fuoss, R. M.; Strauss, U. P. *J. Polym. Sci.* **1948**, *3*, 246.
(3) Pouyet, J. *J. Chem. Phys.* **1951**, *48*, 90.
(4) Butler, J. A. V.; Conway, B. E. *Nature* **1953**, *172*, 153.
(5) Pals, D. T. F.; Hermans, J. J. *Recl. Trav. Chim.* **1952**, *71*, 433.
(6) Eisenberg, H.; Pouyet, J. *J. Polym. Sci.* **1954**, *13*, 85.
(7) Jordon, D. O.; Kuruscev, T. *Polymer* **1960**, *1*, 185.
(8) Hodgson, D. F.; Amis, E. J. *J. Chem. Phys.* **1989**, *91*, 2635.
(9) Nishida, K.; Kaji, K.; Kanaya, T. *Polymer* **2001**, *42*, 8657.
(10) Darskus, R. L.; Jordon, D. O.; Kuruscev, T.; Martin, M. L. *J. Polym. Sci.* **1965**, *A3*, 1941.
(11) Cai, J.; Cheng, R.; Bo, S. *Polymer* **2005**, *46*, 10457.
(12) Vink, H. *Makromol. Chem.* **1970**, *131*, 133.
(13) Vink, H. *J. Chem. Soc., Faraday Trans. 1* **1987**, *83*, 801.
(14) Cohen, J.; Priel, Z.; Rabin, Y. *J. Chem. Phys.* **1988**, *88*, 7111.
(15) Rabin, Y.; Cohen, J.; Priel, Z. *J. Polym. Sci., Part C: Polym. Lett.* **1988**, *26*, 397.
(16) Cohen, J.; Priel, Z. *Polym. Commun.* **1989**, *30*, 223.
(17) Yamanaka, J.; Matsuoka, H.; Kitano, H.; Hasegawa, M.; Ise, N. *J. Am. Chem. Soc.* **1990**, *112*, 587.
(18) Hara, M.; Wu, J. L.; Wang, J.; Jerome, R. J.; Granville, M. *Macromolecules* **1988**, *21*, 3330.
(19) Hara, M.; Wu, J. L.; Wang, J.; Jerome, R. J.; Granville, M. *Polym. Prepr.* **1989**, *30*, 219.
(20) Yamanaka, J.; Matsuoka, H.; Kitano, H.; Ise, N. *J. Colloid Interface Sci.* **1990**, *134*, 92.
(21) Yamanaka, J.; Matsuoka, H.; Kitano, H.; Ise, N.; Yamaguchi, T.; Saechi, S.; Tsubokawa, M. *Langmuir* **1991**, *7*, 1928.
(22) Antonietti, M.; Briel, A.; Forster, S. *J. Chem. Phys.* **1996**, *105*, 7795.
(23) Antonietti, M.; Briel, A.; Forster, S. *Macromolecules* **1997**, *30*, 2700.
(24) Brodwski, G.; Hovath, A.; Ballauff, M.; Rehahn, M. *Macromolecules* **1996**, *29*, 6962.
(25) Reed, W. F. *J. Chem. Phys.* **1994**, *101*, 2515.
(26) Antonietti, M.; Forster, S.; Zisenis, M.; Conrad, J. *Macromolecules* **1995**, *28*, 2270.
(27) Juan, L.; Dougherty, T. J.; Stivala, S. *J. Polym. Sci., Part A−2* **1972**, *10*, 171.
(28) Lovell, A. In *Dilute Solution Viscometry*; Booth, C., Price, C., Eds.; Pergamon Press: London, New York, 1989; p 173.
(29) Yang, Y. *J. Macromol. Sci., Phys.* **2004**, *B43*, 845.
(30) Rushing, T. S.; Hester, R. D. *Polymer* **2004**, *45*, 6587.
(31) Fedors, R. F. *Polymer* **1979**, *20*, 225.
(32) Rao, M. V. S. *Polymer* **1993**, *34*, 592.
(33) Ghimici, L.; Popescu, F. *Eur. Polym. J.* **1998**, *34*, 13.
(34) Dragan, S.; Mihai, M.; Ghimici, L. *Eur. Polym. J.* **2003**, *39*, 1847.
(35) Ghimici, L.; Nichifor, M. *J. Colloid Interface Sci.* **2006**, *302*, 589.
(36) Rotureau, E.; Dellacherie, E.; Durand, A. *Eur. Polym. J.* **2006**, *42*, 1086.
(37) Dragan, S.; Ghimici, L. *Polymer* **2001**, *42*, 2887.
(38) Ghimici, L.; Dragan, S. *Env. Eng. Manag. J* **2002**, *1* (3), 333.
(39) Ghimici, L.; Avram, E. *J. Appl. Polym. Sci.* **2003**, *90*, 465.
(40) Wolf, B. A. *Macromol. Rapid Commun.* **2007**, *28*, 164.
(41) Eckelt, J.; Knopf, A.; Wolf, B. A. *Macromolecules* **2008**, *41*, 912.
(42) Nichifor, M.; Lopes, S.; Bastos, M.; Lopes, A. *J. Phys. Chem. B* **2004**, *108*, 16463.
(43) Pass, G.; Hales, P. W. In *Solution Properties of Polysaccharides*; Brant, D. A., Ed.; ACS Symposium Series 150; American Chemical Society: Washington, DC, 1981; p 349.
(44) Manning, G. S. *J. Chem. Phys.* **1969**, *51*, 924.
(45) Manning, G. S. *J. Phys. Chem.* **1975**, *79*, 262.
(46) Geerissen, H.; Schmidt, J. R.; Wolf, B. A. *J. Appl. Polym. Sci.* **1982**, *27*, 1277.
(47) Stevens, M.; Kremer, K. *J. Chem. Phys.* **1995**, *103*, 1669.
(48) Schiessel, H.; Pincus, P. *Macromolecules* **1998**, *31*, 7953.

JP900690F